EUROPEAN ORGANIZATION FOR NUCLEAR RESEARCH

L3 Note 2771
July 22, 2002

Study of the $e^-e^+ \to Ze^-e^+$ process at LEP

The L3 Collaboration

Abstract

The cross section of the process $e^-e^+ \to Ze^-e^+$ is measured with $0.7\,\mathrm{fb}^{-1}$ of data collected with the L3 detector at LEP. Hadronic decays of the Z boson are considered at centre-of-mass energies ranging from 183 GeV up to 209 GeV. The results are found to be in agreement with Standard Model predictions. These results are PRELIMINARY.

To be submitted to *31^st International Conference on High Energy Physics*
Amsterdam, the Netherlands, 24-31 July 2002.

Introduction

The study of the pair-production of Z and W bosons in e^+e^- collisions constitutes one of the main subjects of the scientific program carried out at the LEP machine. In addition to these s- and t-channel processes, a "single" weak gauge boson can also be produced via t-channel diagrams. A common feature of this single boson production is the emission of a virtual photon off the incoming electron or positron, which is almost unscattered at very low polar angles and hence not detected. Particular care has to be exercised when predicting the cross sections of these processes, due to the running of the electromagnetic coupling of the photon, and the peculiarities of the modelling of small angle scattering. The comparison of these predictions with experimental data is made more interesting by the fact that the single boson production is a copious source of bosons at higher centre-of-mass energies. The "single W" production is extensively studied at LEP [1, 2] and this note concentrates on "single Z" production.

Figure 1 presents two Feynman diagrams for the single Z production, followed by the decay of the Z into a quark-antiquark pair. A peculiarity of the process is the photon-electron scattering, reminiscent of the Compton scattering. These diagrams are only an example of the 48 contributing to the $e^+e^- \to e^+e^-q\bar{q}$ process. The single Z signal is defined starting from this full set of diagrams, excluding QCD contributions from two-photon physics, and applying some kinematical cuts:

$$m_{q\bar{q}} > 60 \text{ GeV}, \;\; \theta_{unscattered} < 12^\circ, \;\; 60^\circ < \theta_{scattered} < 168^\circ, \;\; E_{scattered} > 3.0 \text{ GeV}, \qquad (1)$$

where $m_{q\bar{q}}$ refers to the invariant mass of the quark antiquark pair produced, $\theta_{unscattered}$ is the polar angle at which the electron[1)] closest to the beam line is emitted, $\theta_{scattered}$ and $E_{scattered}$ are respectively the polar angle with respect to its incoming direction and the energy of the electron scattered at the largest polar angle.

These criteria largely enhance the contribution diagrams similar to those in Figure 1 over the remaining phase space of the $e^+e^- \to e^+e^-q\bar{q}$ process and correspond to a cross section of about 0.6 pb at a centre-of-mass energy $\sqrt{s} = 200$ GeV.

This note describes the selection of $e^+e^- \to Ze^+e^- \to e^+e^-q\bar{q}$ events in the data sample collected by the L3 detector at LEP and the measurement of the cross section of this process. Results at lower centre of mass energy were previously reported [1, 3].

Data and Monte Carlo samples

This analysis is based on 675.5 pb^{-1} of integrated luminosity collected by the L3 detector [4] at LEP at $\sqrt{s} = 182.7 - 209.0$ GeV. This sample is divided in eight different energy bins whose corresponding values of average $\sqrt{s}$ and integrated luminosity are reported in Table 1.

$\sqrt{s}$ [GeV]	182.7	188.6	191.6	195.5	199.5	201.7	204.9	206.6
$\mathcal{L}$ [pb^{-1}]	55.1	176.0	29.4	83.0	80.8	36.7	76.6	137.9

Table 1: The average centre-of-mass energies and the corresponding integrated luminosities used in this study.

1) The word "electron" is used for both the electrons and positrons.

The signal process is modelled with WPHACT Monte Carlo program [5]. The GRC4F [6] event generator is used for systematic checks. Events are generated in a phase space broader than the one defined by the criteria (1). Events that do not satisfy these criteria are considered as background. The $\mathrm{e^+e^-} \rightarrow \mathrm{q\bar{q}}(\gamma)$ process is simulated with the KK2f [7] Monte Carlo generator, $\mathrm{e^+e^-} \rightarrow \mathrm{ZZ}$ with PYTHIA [8], and $\mathrm{e^+e^-} \rightarrow \mathrm{W^+W^-}$ process, with the exception of $\mathrm{q\bar{q}'e}\nu$ final state, with KORALW [9]. EXCALIBUR [10] is used to simulate the $\mathrm{q\bar{q}'e}\nu$ and other four-fermion final states. Hadron production in two-photon interactions is modelled with PHOJET [11]. The generated events are passed through the L3 detector simulation program [12]. Time dependent detector inefficiencies, as monitored during the data taking period, are also reproduced.

Event Selection

The event selection proceeds from high multiplicity events with at least one isolated electron identified in the BGO electromagnetic calorimeter, with energy in excess of 3 GeV. To strongly suppress the contribution from the high cross section background processes, the signal topology is enforced requiring events with an invariant mass of the hadronic system, stemming from a Z boson, between 50 and 130 GeV, a visible energy of at least $0.4\sqrt{s}$ and a missing momentum, due to the undetected electron, of at least $0.24\sqrt{s}$. After these selection criteria, 1551 events are selected in the full data sample. From Monte Carlo, 1550 ± 4 events are expected, out of which 208 ± 1 are signal events with an efficiency of 57% and a purity of 13%. Most of the background arises from the $\mathrm{e^+e^-} \rightarrow \mathrm{q\bar{q}'e}\nu$ (63%), $\mathrm{e^+e^-} \rightarrow \mathrm{q\bar{q}}(\gamma)$ (20%) and $\mathrm{e^+e^-} \rightarrow \mathrm{W^+W^-}$ (12%) processes.

The particular signature of an electron undetected at low angle and the other scattered in the detector allows to reject a large fraction of the background by considering two powerful kinematic variables: the product of the charge, q, of the detected electron and its polar angle, $\cos\theta$, and the product of q and the polar angle of the direction of the missing momentum, $\cos\not\theta$. Two selection criteria are applied:

$$q \times \cos\theta > 0.5 \ \text{ and } \ q \times \cos\not\theta > 0.94.$$

The effect of these criteria is presented in Figure 2. In addition, the event is forced in two jets by means of the DURHAM algorithm [13], and the opening angle between the two jets is required to exceed 150°. Few more background events are rejected by tightening the electron isolation criteria. Table 2 summarises the yield of the event selection.

Results

Figure 3 presents the distribution of the invariant mass of the hadronic system after all selection cuts are applied. A large signal around the mass of the Z boson is observed. The single Z cross sections at each value of $\sqrt{s}$ are determined from a maximum-likelihood fit to the distribution of this variable. The results are listed in Table 3, together with the prediction of the WPHACT Monte Carlo.

Several possible sources of systematic uncertainty are considered and their effects on the measured cross sections are listed in Table 4. First, detector effects and the accuracy of the Monte Carlo simulation are investigated by varying the energy scale of the calorimeter, the amount of charge confusion in the tracker, visible in Figure 2, and the selection criteria. The

$\sqrt{s}$ [GeV]	ε [%]	N_{Data}	N_{MC}	N_{Sign}	$N_{\mathrm{q\bar{q}}(\gamma)}$	$N_{\mathrm{e}\nu\mathrm{q\bar{q}'}}$	$N_{\mathrm{two-phot}}$
182.7	42.3	16	16.0 ± 0.3	12.0 ± 0.1	0.4	3.2	0.2
188.6	42.7	53	52.4 ± 0.9	40.3 ± 0.4	0.5	9.5	1.0
191.6	43.0	9	8.7 ± 0.2	6.9 ± 0.1	0.0	1.3	0.3
195.5	45.0	19	26.5 ± 0.4	21.2 ± 0.1	0.0	3.6	1.1
199.5	45.2	18	27.1 ± 0.5	21.3 ± 0.1	0.4	3.8	1.2
201.7	44.0	16	12.2 ± 0.4	9.5 ± 0.2	0.3	1.6	0.5
204.9	43.3	24	24.6 ± 0.3	19.9 ± 0.2	0.2	2.9	1.1
206.6	44.6	47	46.2 ± 0.7	37.2 ± 0.3	0.3	5.4	2.2

Table 2: Yield of the event selection at the different centre-of-mass energies. The signal efficiency, ε, is listed together with the number of observed, N_{Data}, and total expected, N_{MC}, events. The expected number of signal events, N_{Sign}, is given together with indications on the most important residual backgrounds, respectively indicated with $N_{\mathrm{q\bar{q}}(\gamma)}$, $N_{\mathrm{e}\nu\mathrm{q\bar{q}'}}$ and $N_{\mathrm{two-phot}}$ for the processes $\mathrm{e^+e^-} \rightarrow \mathrm{q\bar{q}}(\gamma)$, $\mathrm{e^+e^-} \rightarrow \mathrm{e}\nu\mathrm{q\bar{q}'}$ and the hadron production in two-photon interactions.

$\sqrt{s}$ [GeV]	$\sigma^{\mathrm{Measured}}$ [pb]	$\sigma^{\mathrm{Expected}}$ [pb]
182.7	$0.51^{+0.19}_{-0.16} \pm 0.03$	0.51
188.6	$0.54^{+0.10}_{-0.16} \pm 0.03$	0.54
191.6	$0.60^{+0.26}_{-0.21} \pm 0.03$	0.55
195.5	$0.40^{+0.13}_{-0.11} \pm 0.02$	0.56
199.5	$0.33^{+0.12}_{-0.10} \pm 0.02$	0.58
201.7	$0.81^{+0.26}_{-0.22} \pm 0.04$	0.59
204.9	$0.55^{+0.16}_{-0.14} \pm 0.03$	0.60
206.6	$0.59^{+0.12}_{-0.10} \pm 0.03$	0.61

Table 3: Measured and expected cross sections at the different centre-of-mass energies. The first uncertainties are statistical and the second systematic. Expectations are calculated with the WPHACT Monte Carlo program.

impact of the signal modelling on the final efficiencies is studied by using the GRC4F Monte Carlo program instead of the WPHACT event generator. The expected cross sections of the background processes are varied of 10%, 5%, 1% and 100% respectively for the $\mathrm{e^+e^-} \rightarrow \mathrm{q\bar{q}}(\gamma)$, $\mathrm{e^+e^-} \rightarrow \mathrm{e}\nu\mathrm{q\bar{q}'}$, $\mathrm{e^+e^-} \rightarrow \mathrm{W^+W^-}$ processes and the hadron production in two-photon interactions. Finally, the effects of the limited background and signal Monte Carlo statistics are considered.

Figure 4 compares the results of the measurement of the cross section of the process $\mathrm{e^+e^-} \rightarrow \mathrm{Ze^+e^-} \rightarrow \mathrm{q\bar{q}e^+e^-}$ with both the WPHACT and the GRC4F predictions. A good agreement is observed. This agreement is quantified by extracting the ratio R between the measured cross sections $\sigma^{\mathrm{Measured}}$ and the WPHACT predictions $\sigma^{\mathrm{Expected}}$:

$$R = \frac{\sigma^{\mathrm{Measured}}}{\sigma^{\mathrm{Expected}}} = 0.88 \pm 0.08 \pm 0.06,$$

where the first uncertainty is statistical and the second systematic.

Source	Systematic uncertainty
Energy scale	2.3%
Charge confusion	0.8%
Cut variation	4.4%
Signal modelling	1.2%
Background modelling	1.9%
Background Monte Carlo statistics	1.4%
Signal Monte Carlo statistics	0.9%
Total	5.7%

Table 4: Sources of systematic uncertainties.

In conclusion, the process $e^+e^- \rightarrow Ze^+e^- \rightarrow q\bar{q}$ has been studied at LEP and its cross section measured and found to agree with theory calculation based on Monte Carlo programs, validating these prediction with an experimental accuracy of 10%.

References

[1] DELPHI Collab.,P. Abreu *et al.*, Phys. Lett. **B 515** (2001) 238 .

[2] ALEPH Collab., R. Barate *et al.*, Phys. Lett. **B 462** (1999) 389; ALEPH Collab.,A. Heister *et al.*, Eur. Phys. J. **C 21** (2001) 423; DELPHI Collab., P. Abreu *et al.*, Phys. Lett. **B 459** (1999) 382; DELPHI Collab.,P. Abreu *et al.*, Phys. Lett. **B 502** (2001) 9; L3 Collab. M. Acciarri *et al.*, Phys. Lett. **B 403** (1997) 168; L3 Collab. M. Acciarri *et al.*, Phys. Lett. **B 436** (1998) 417; L3 Collab. M. Acciarri *et al.*, Phys. Lett. **B 487** (2000) 229; L3 Collab. L3 note 2753 (2002) .

[3] OPAL Collab. G. Abbiendi *et al.*, Phys. Lett. **B 438** (1998) 391; OPAL Collab. G. Abbiendi *et al.*, Eur. Phys. J. **C 24** (2002) 1 .

[4] L3 Collab., B. Adeva et al., Nucl. Instr. Meth. **A 289** (1990) 35; O. Adriani et al., Phys. Reports **236** (1993) 1; M. Chemarin et al., Nucl. Instr. Meth. **A 349** (1994) 345; M. Acciarri et al., Nucl. Instr. Meth. **A 351** (1994) 300; G. Basti et al., Nucl. Instr. Meth. **A 374** (1996) 293; I.C. Brock et al., Nucl. Instr. Meth. **A 381** (1996) 236; A. Adam et al., Nucl. Instr. Meth. **A 383** (1996) 342 .

[5] WPHACT version 2.1; E. Accomando and A. Ballestrero, Comp. Phys. Comm. **99** (1997) 270; E. Accomando, A. Ballestrero and E. Maina, preprint hep-ph/0204052 (2002) .

[6] GRC4F version 2.1; J. Fujimoto *et al.*, Comp. Phys. Comm. **100** (1997) 128 .

[7] KK2f version 4.13; S. Jadach, B.F.L. Ward and Z. Wąs, Comp. Phys. Comm. **130** (2000) 260 .

[8] PHYTHIA version 5.772 and JETSET version 7.4; T. Sjöstrand, Preprint CERN-TH/7112/93 (1993), revised 1995; T. Sjöstrand, Comp. Phys. Comm. **82** (1994) 74 .

[9] KORALW version 1.33; M. Skrzypek *et al.*, Comp. Phys. Comm. **94** (1996) 216; M. Skrzypek *et al.*, Phys. Lett. **B 372** (1996) 289 .

[10] F.A. Berends, R. Pittau and R. Kleiss, Comp. Phys. Comm. **85** (1995) 437 .

[11] PHOJET version 1.05; R. Engel, Z. Phys. **C66** (1995) 203; R. Engel, J. Ranft and S. Roesler, Phys. Rev. **D52** (1995) 1459 .

[12] The L3 detector simulation is based on GEANT 3.21, see R. Brun et al., CERN report CERN DD/EE/84-1 (1984), revised 1987, and uses GHEISHA to simulate hadronic interactions, see H. Fesefeldt, RWTH Aachen report PITHA 85/02 (1985) .

[13] S. Bethke *et al.*, Nucl. Phys. **B 370** (1992) 310, and references therein .

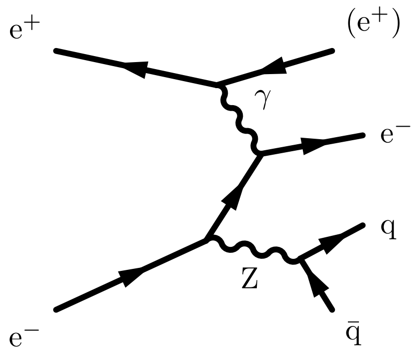

Figure 1: Diagrams contributing to the "Single Z" production.

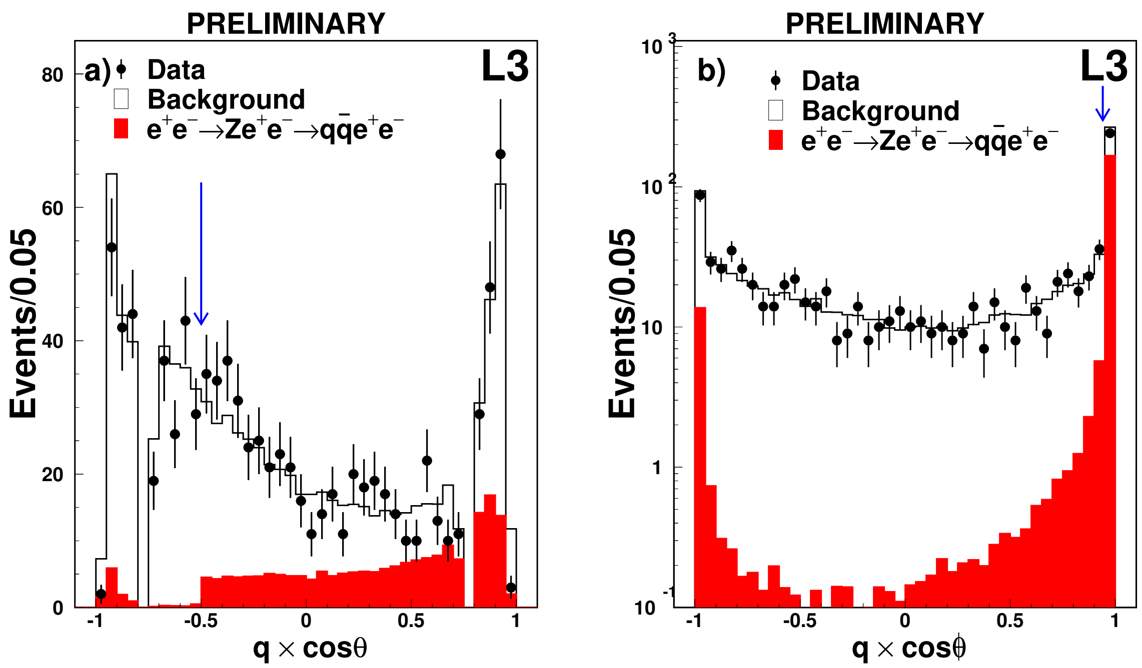

Figure 2: Distributions for data, signal and background Monte Carlo of the product of the charge of the detected electron and a) the cosine of its polar angle and b) the cosine of the polar angle of the missing momentum. The arrows show the position of the applied cuts. All other selection criteria but those on these two variables are applied. Signal events around -1 correspond to charge confusion in the central tracker.

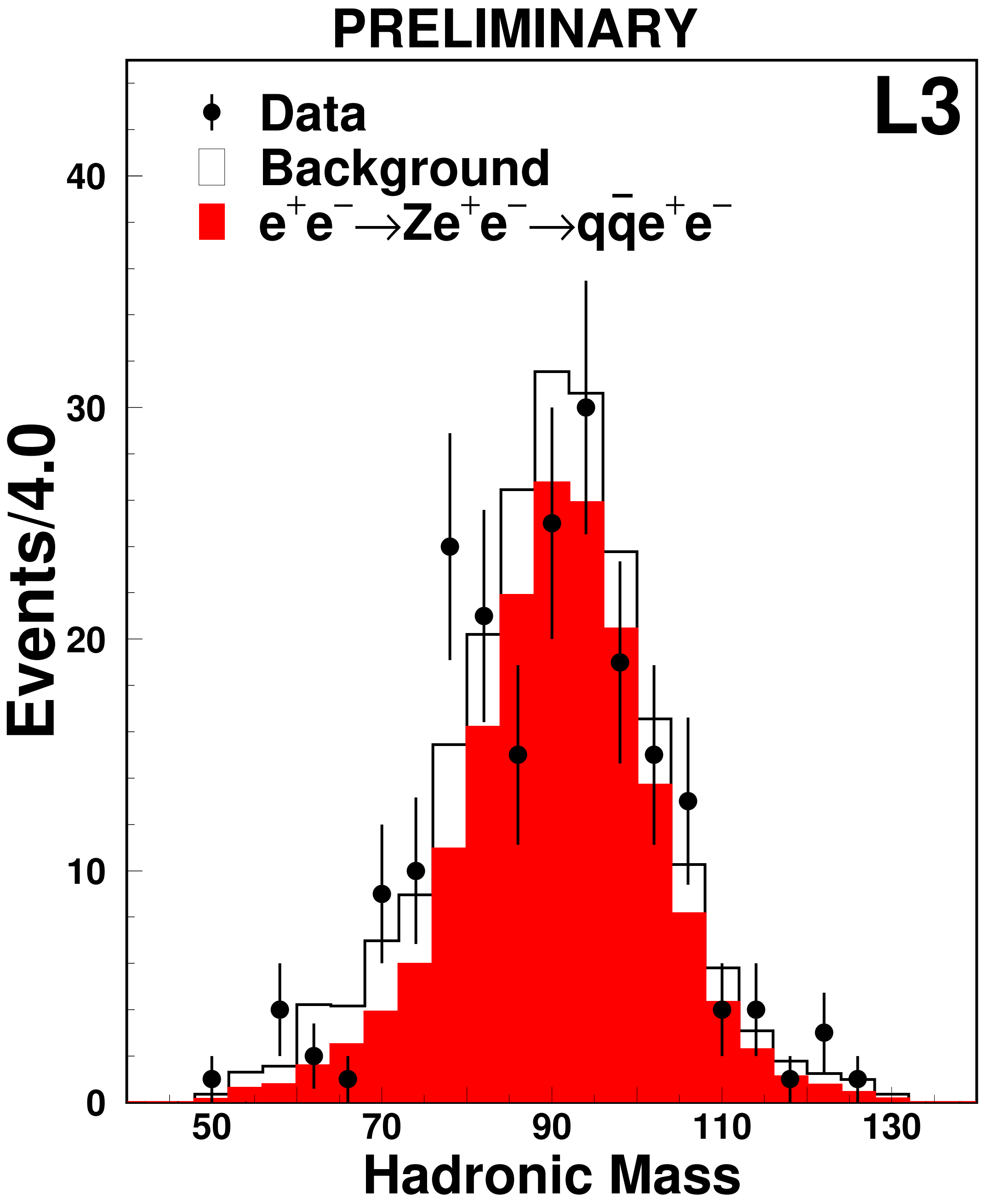

Figure 3: Distribution of the invariant mass of the hadronic system for events selected in data, signal and background Monte Carlo.

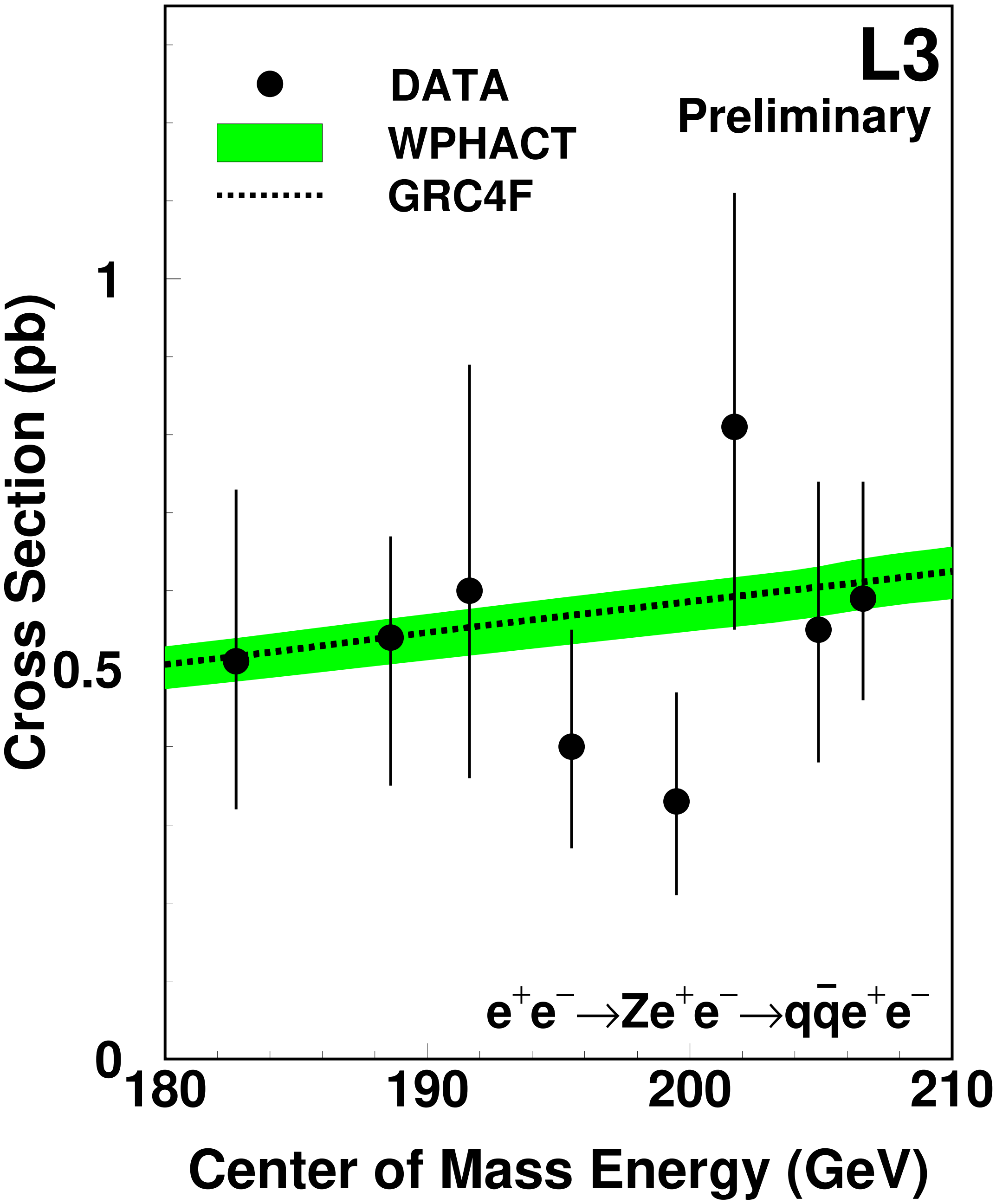

Figure 4: Measurements of the cross section of the $e^+e^- \rightarrow Ze^+e^-q\bar{q}$ process as a function of the centre-of-mass energy. The WPHACT predictions are assigned an uncertainty of 5